Research Article

Copper Corrosion Inhibition by Tyrosine Amino-Acid in Nitric Acid Solution

Khadija Barouni, Abdelbaki Kassale, Lahcen Bazzi*, Abdollah Albourine
Materials and Environmental Laboratory, Faculty of Sciences, Ibn Zohr University Agadir Morocco

Abstract

The inhibiting action of tyrosine (Tyr) on the corrosion inhibitor of copper in nitric acid solution has been studied by using weight loss, electrochemical polarization, and scanning electron microscopy (SEM) measurements. The effect of inhibitor concentration, temperature and immersion time against inhibitor action was investigated. The experimental results suggest that Tyr at 10^{-3}M is a good corrosion inhibitor for copper in nitric acid at temperature 20°C. Results obtained from weight loss and potentiodynamic polarization measurements are in good agreement. Potentiodynamic polarization studies reveal that Tyr acts as a cathodic inhibitor without any change in the mechanism of hydrogen evolution. The adsorption of this compound onto the copper surface was found to follow the Langmuir adsorption isotherm. The corrosion inhibition is due to the formation of a chemisorbed film on the copper surface. The electronic properties of Tyr, obtained using the AM1 and MNDO Semi-empirical quantum chemical approach, have been correlated with their experimental inhibition efficiencies.

Keywords: Corrosion, Inhibition, Copper, Tyrosine, Nitric acid, Polarisation, Quantum chemical calculations

***Correspondence**
Author: lahcen bazzi
Email: bazzilahcen@gmail.com

Introduction

Copper has an excellent thermal conductivity, good mechanical workability, and relatively noble properties [1]. It is a material commonly used in heating and cooling systems, and it is also used for electricity transportation due to its high conductance [2-4]. Scale and corrosion products have a negative effect on heat transfer, causing a decrease in heating efficiencies of the equipment, which is why periodic descaling and cleaning in acid pickling solutions are necessary [5]. One of the most important methods in the protection of copper against corrosion is the use of inhibitors [6-9]. Corrosion inhibitors effectively eliminate the undesirable destructive effect and prevent copper dissolution. There are various types of organic inhibitor that tend to decrease the corrosion rate of copper in acidic solutions [10-24]. In general organic compounds containing polar group (carboxylic/amino acids) including nitrogen, sulfur and oxygen atoms [25-31] and heterocyclic compounds with polar functional groups and conjugated double bonds [31, 32] have been reported to inhibit the corrosion of copper. The inhibiting action of these organic compounds is usually attributed to their interactions with the copper surface via their adsorption [6]. However, the adsorption of an inhibitor on a metal surface depends mainly on the electronic and structural properties of the inhibitor molecule [33]. Unfortunately, many common corrosion inhibitors are highly toxic and health-hazardable for the inhibition of corrosion in aqueous media [34]. Our research was aimed at making organic compounds with low toxicity and good inhibition efficiency against copper corrosion. Amino acids with non-toxic characteristics have been tested as inhibitors of copper [2, 26, 28, 31], Al [35] and mild steel [36, 37] corrosion in acidic media. They are relatively easy to produce with high purity at low cost and are completely soluble in aqueous media. The object of this study is to investigate the inhibition of Tyr as corrosion for copper in molar acid nitric by use of electrochemical polarization measurements and weight-loss measurements. The adsorption of Tyr onto copper surface was studied to determine the appropriate adsorption isotherm, the standard free energies of adsorption ($\Delta G°ads$) and some thermodynamic data. The quantum chemical method was also employed to optimize the geometry and to calculate the energy of their front molecular orbital, energy gap, and net atomic charge for further discussion on the relationship between inhibitory effect and quantum parameters of the inhibitors.

Experimental

Materials and Reagents

The copper working was of 99% purity. The aggressive solution of 1 mol L^{-1} HNO_3 was prepared by dilution of Analytical Grade 65% of mark Taoura with bidistilled water. The specimens used in the gravimetric tests have a rectangular form with face whose total surface is $12cm^2$. For the electrochemical measurements were performed in a conventional three electrodes electrochemical cell. Consisting of platinum electrode, as an Auxiliary electrodes, saturated calomel electrode (SCE), as the reference and Cu metal as the working electrode, it had the form of a disc from pure copper of the surface 0.35 cm^2. Before the measurements the copper specimens were polished successively with emery paper up to 1000 grade, rinsed thoroughly with acetone and bidistilled water. Pure copper was immersed in molar HNO_3 at various concentrations of Tyr (10^{-5} to 10^{-2}mol L^{-1}).The amino acid compound tested as inhibitor is the commercial product. The structural formula is shown in **Figure 1**.

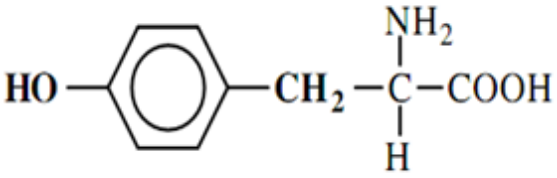

Figure 1 The molecular structure of Tyr

Gravimetric and electrochemical measurements

Gravimetric measurements were made in intervals of 2, 4, 16 and 24 hours. All experiments were carried out under total immersion in 75 ml of test solutions at temperature 20°C. Mass loss was recorded by an analytical balance with 0.1mg. The surface morphology of the specimens after 24 hours in 1.0 mol/L HNO_3 solution in the absence and presence of 10^{-3}mol/L of Tyr at 20°C obtained from weight loss measurements were tested on a scanning electron microscopy (SEM). The polarization experiments were conducted with a potentiostat PGP 201 associated to "Volta Master 1". The polarization curves were obtained by means of the linear potential sweep of 1mV/s after the working electrode was left under free corrosion (for about 30 min) to reach a stable potential. The potential ranged from -800 to +500mV/SCE.

Quantum chemical method

The semi-empirical computational methods have been used most successfully in finding correlation between theoretically calculated properties and experimentally determined inhibition efficiency for uniform corrosion [38, 39].The computation of the energies of the molecules, EHOMO (highest occupied molecular orbital), ELUMO (lowest unoccupied molecular orbital) and energy gap (ΔE=ELUMO−EHOMO) and the electronic charges on reactive centres of the Tyr had been performed using the AM1 (Austin Model 1) [40] and MNDO (modified neglect of differential overlap) [41], semi-empirical methods implemented in MOPAC6.0 program [42].

Results and discussions

Effect of Concentration of Tyr

Figure 2 shows the influence of Tyr concentration on the cathodic and anodic polarisation curves of copper in 1 mol.L^{-1} HNO_3. **Table 1** gives values of corrosion current (I_{corr}), corrosion potential (E_{corr}), cathodic Tafel slope (b_c). In this case, the relation determines the inhibition efficiency (E_I %):

$$E_I(\%) = \left(1 - \frac{I'_{cor}}{I_{cor}}\right) \times 100$$

Where I_{corr} and I'_{corr} are the uninhibited and inhibited corrosion current densities, respectively, determined by extrapolation of cathodic Tafel lines to corrosion potential.

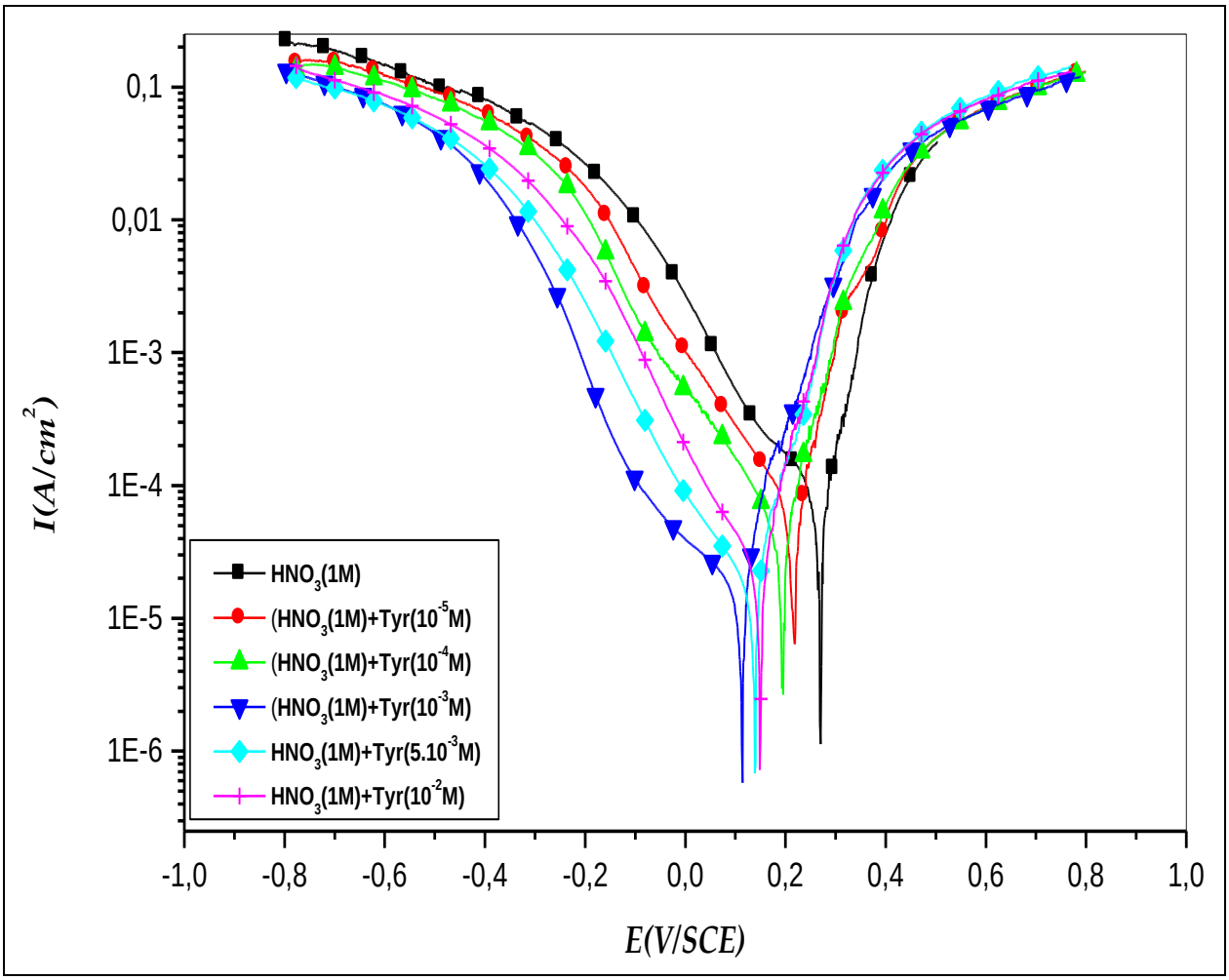

Figure 2 Polarization curves for the effect of Tyr concentration on the potentiodynamic behaviour of pure copper in 1.0 mol.L^{-1} HNO_3 (T=20°C).

Table 1 Electrochemical Parameters Derived from Figure 1

Solutions	[C] (mol/l)	E_{corr} (mV/SCE)	I_{corr} (µA/cm^2)	bc (mV/dec.)	R_p (Ω.cm^2)	E_I (%)	E_{Rp} (%)
HNO_3 (1M)	0	261	84	-163	5263	---	---
HNO_3 (1M) + [Tyr]=C	10^{-5}	218	57	-165	7628	32	31
	10^{-4}	195	47	-165	9251	44	43
	10^{-3}	111	15	-160	28653	82	82
	5.10^{-3}	140	18	-161	24155	78	78
	10^{-2}	151	22	-161	19763	74	73

As it is shown in Figure 2, cathodic polarisation curves rise to parallel Tafel lines indicating that the hydrogen evolution reaction is activation controlled. Thus, the presence of Tyr compound does not affect the mechanism of this process [2, 43-45]. Table 1 show that the values of I_{corr} decrease with the rise of Tyr concentration. We note that the corrosion current densities were significantly reduced in the presence of Tyr and became only 15µAcm^{-2} at 10^{-3} M. The addition of Tyr shifted the E_{corr} value towards the negative direction. This indicates that the inhibitor compound

used controls predominantly the cathodic reaction and acts as a cathodic inhibitor [46]. The same results have been reported by other authors [6, 47]. The values of cathodic Tafel slope (b_c) remain almost constant upon the addition of inhibitor concentration. The results demonstrate that the hydrogen reduction is inhibited and that the inhibition efficiency increases with inhibitor concentration to attain 82% at 10^{-3} mol.L^{-1} and then decreases at higher concentrations and reach a 73% at 10^{-2} mol.L^{-1}.

The essential effect of corrosion inhibition is attributed to the presence of NH_2, C=O and OH groups and the presence of aromatic ring in molecule, which have a strong affinity for copper.

It is noticed that presence of heteroatoms such as nitrogen, sulphur, phosphorous in the organic compound molecule improves its action as copper corrosion inhibitor [2, 48-49]. Interaction with rings containing conjugated bonds, π electrons, is also present. This is explained by the presence of vacant d orbitals in copper atom that form coordinative bonds with atoms able to donate electrons [33] and also, the presence of pairs of free electrons on nitrogen and oxygen atoms and of electrons in aromatic rings favours adsorption of Tyr and, thus, the best efficiency of this inhibitor [25, 48].

The corrosion parameters such as the values of polarization resistance R_p of copper in 1 mol.L^{-1} HNO_3 without and in the presence of various concentrations of inhibitor and corresponding inhibition efficiencies (E_{Rp}%) are shown in Table 1. In this method, the inhibition efficiency can be calculated by the relation:

$$E_{Rp} = \frac{Rp'-Rp}{Rp'} \times 100$$

Where R'_P and R_P are the polarisation resistance values with and without the inhibitor, respectively.

We remark that the polarization resistance (R_P) values increases with the rise of Tyr concentration. However, R_p related to the copper in 1 M HNO_3 is the lower value. This result was accompanied with an increase of the inhibition efficiencies and attains a maximum value (82%) at 10^{-3} mol.L^{-1}.

Adsorption isotherm

The dependence of the fraction of the surface covered obtained by the ratio E/100 as function of the logarithm of the concentration (log(C)) of Tyr was tested graphically by fitting it to several adsorption isotherms. The best description of the adsorption behaviour of Tyr was the Langmuir adsorption isotherm, which obeys [50]:

$$\frac{C}{\theta} = \frac{1}{K} + C$$

Where **C** is the inhibitor concentration, **K** is the equilibrium constant of the adsorption process, and **θ** is the fraction of the surface covered determined by E/100.

Figure 3 shows the dependence of the ratio C/θ as function of the concentration of Tyr. The obtained plot of Tyr is linear with a slope equal to 1.34. The regression coefficient is R = 0.9992. The intercept permits the calculation of the equilibrium constant K which is 30258.56 which leads to evaluate ΔG_{ads} = -35 kJ.mol^{-1} (**Table 2**). The large negative value of ΔG_{ads} indicated that Tyr was strongly adsorbed on the copper surface [51].Generally, values of ($\Delta G_{ads}°$) up to -20 kJ mol^{-1} are consistent with the electrostatic interactions between the charged molecules and the charged metal (physisorption) while those around -40 kJ mol^{-1} or higher are associated with chemisorption as a result of sharing or transfer of electrons from organic molecules to the metal surface to form a coordinate type of bond (chemisorption) [52]. The calculated $\Delta G°_{ads}$ value of slightly more negative than - 30 kJ mol^{-1} indicate, therefore, that the adsorption mechanism of the investigated Tyr on copper in 1M HNO_3 solution is typical of chemisorption [31, 33, 53-56]. The possible mechanisms for chemisorption can be attributed to the donation π-electron by the aromatic rings, the nonbinding electron pair of the oxygen and nitrogen atoms in hydroxide and amine groups respectively favors the adsorption of the inhibitor on the metal surface [52].

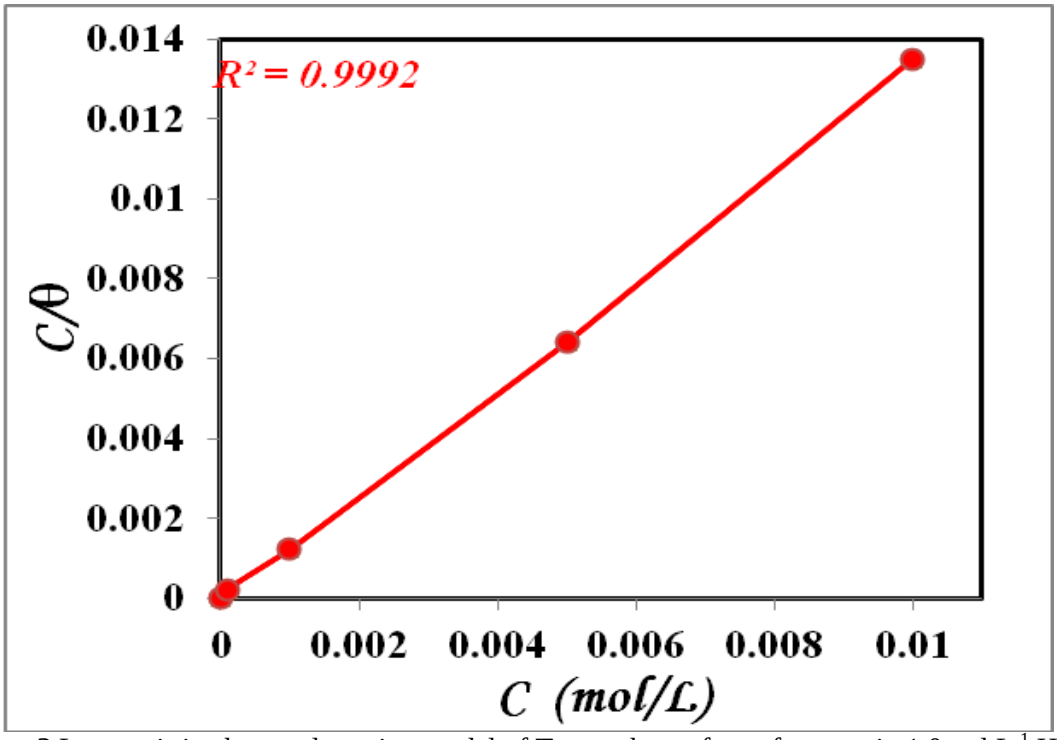

Figure 3 Langmuir isotherm adsorption model of Tyr on the surface of copper in 1.0mol.L^{-1} HNO_3

Table 2 Equilibrium constant adsorption linear, correlation coefficient and standard free energy of the adsorption for copper in 1.0 mol.L^{-1} HNO_3 solution in the presence of Tyr

Inhibiteur	K	R^2	$\Delta G°_{ads}$ (Kj/mol)
Tyr	**30258.56**	**0.9992**	**-35**

Effect of the Temperature

Wight-Loss Measurements

Temperature has a great effect on the corrosion phenomenon. Generally the corrosion rate increases with the rise of the temperature [54]. For this purpose, we made weight-loss measurements in the range of temperature 20 to 50°C, in the absence and presence of Tyr at 10^{-3} mol.L^{-1} after 4h of immersion. The corresponding data are shown in **Table 3**. It is clear that the increase of corrosion rate is more pronounced with the rise of temperature for the blank solution. In the presence of the inhibitor, V_{corr} is reduced even at high temperature (**Figure 4**). **Figure 5** displays the variation of the inhibitor efficiency (E%) at different temperatures. It was observed that inhibition efficiency decreases when the temperature increases. E (%) passed from 83 to 22% when temperature rises from 20 to 50°C at 10^{-3} mol/L of Tyr. We note that the efficiency of the inhibitor tested depend on the temperature and decreases with the rise of temperature from 20 to 50°C [54].

Table 3 Effect of Temperature on the Cu Corrosion in Molar HNO_3 and Added of 10^{-3} mol L^{-1} of Try

Solution	T (°C)	V_{corr} (mg/h.cm^2)	V'_{corr} (mg/h.cm^2)	E_G(%)
HNO_3 (1M) + Tyr (10^{-3}M)	20	0.054	9.35	83
	30	0.10	52	48
	40	0.23	150	35
	50	2.41	1880	22

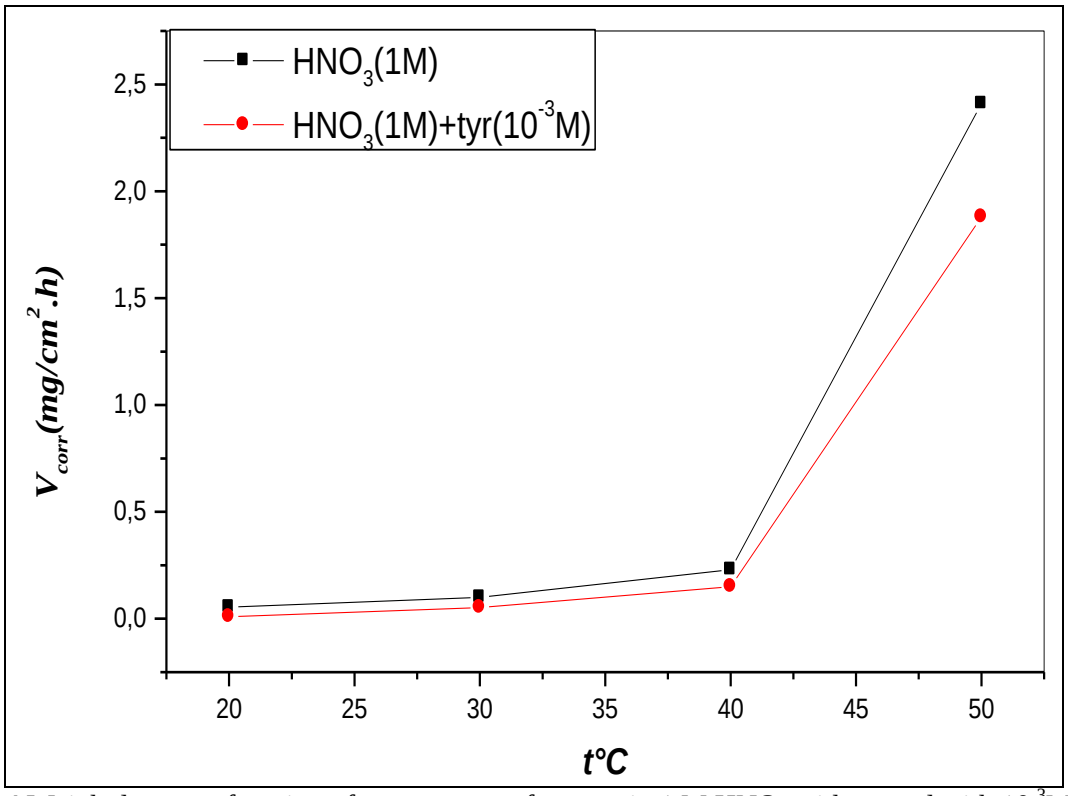

Figure 4 Weight loss as a function of temperature of copper in 1 M HNO_3 without and with 10^{-3}M of Tyr

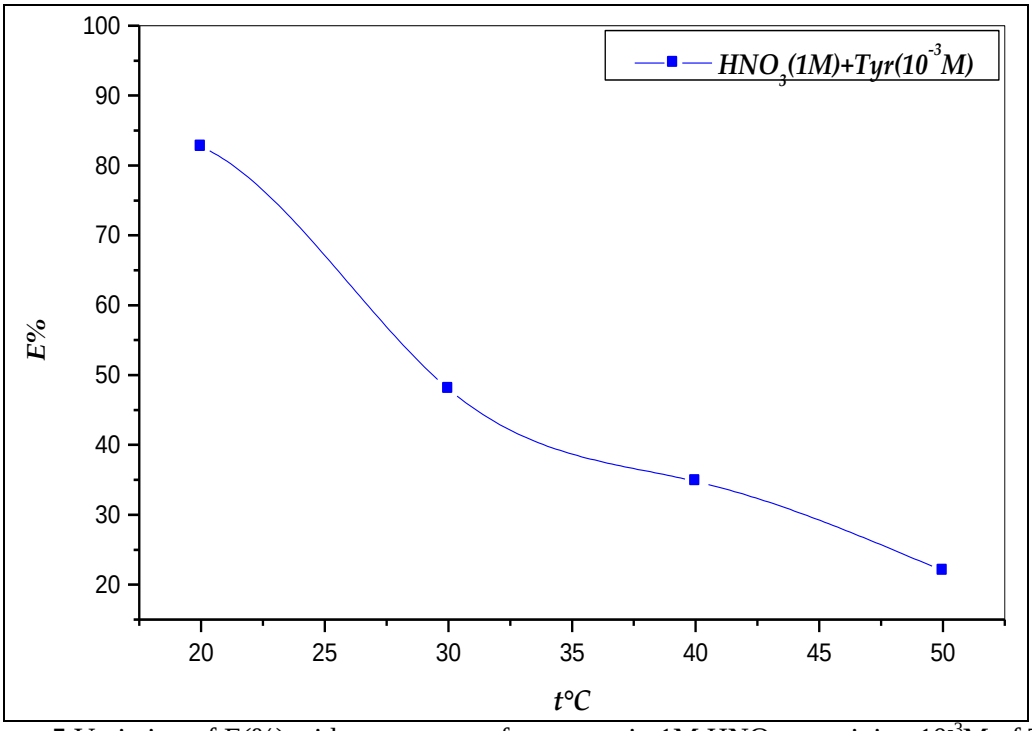

Figure 5 Variation of E(%) with temperature for copper in 1M HNO_3 containing 10^{-3}M of Tyr

Polarization Measurements

Figure 6 shows the polarization curves for pure copper in molar HNO_3 solutions without and with Tyr at 10^{-3} mol.L^{-1} at different temperatures. The corresponding values of the electrochemical parameters are shown in **Table 4**.

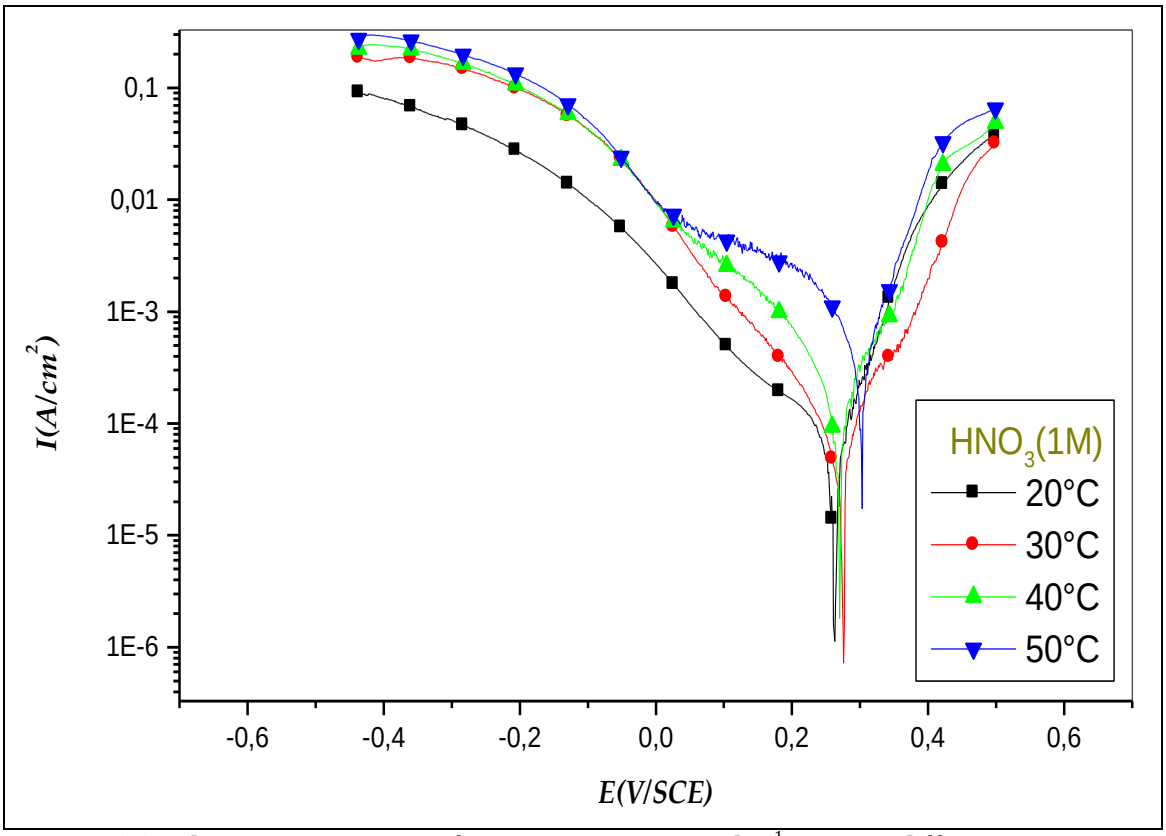

Figure 6 (**a**) Polarisation curves I-E of pure copper in: 1.0 mol L^{-1} HNO_3 at different temperatures

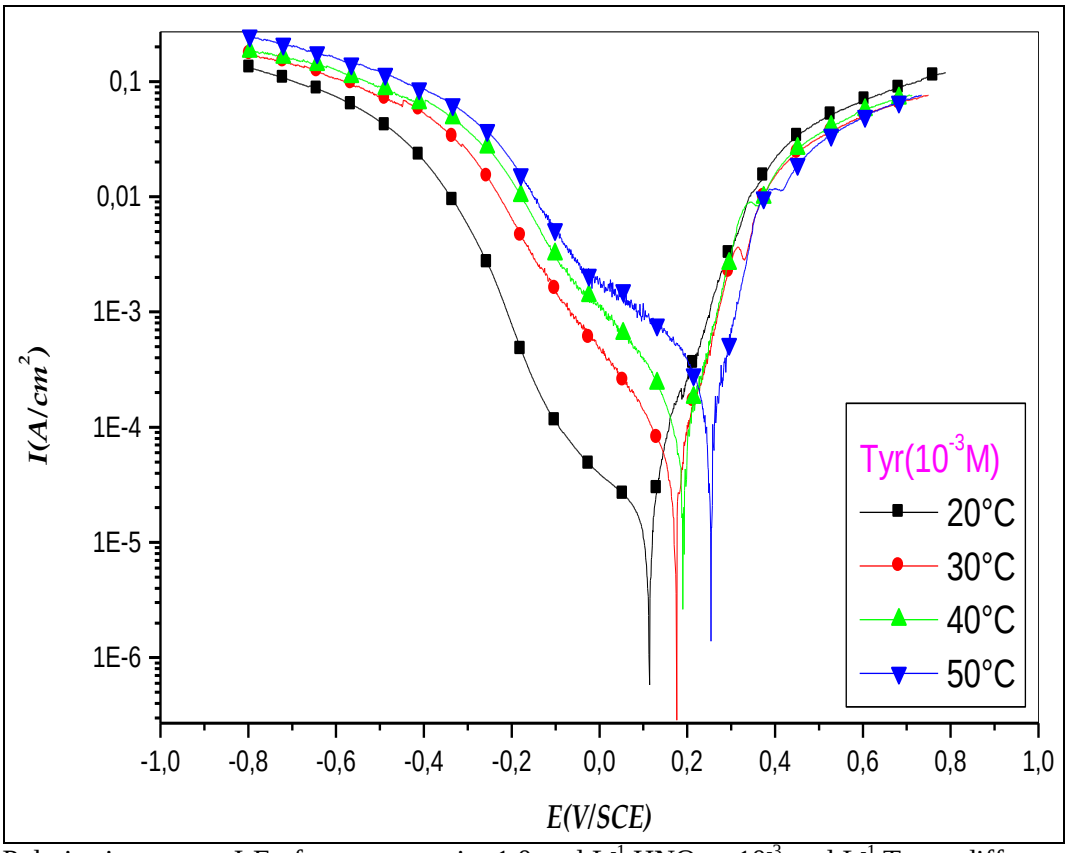

Figure 6 (b) Polarisation curves I-E of pure copper in: 1.0 mol L^{-1} HNO_3 + 10^{-3} mol L^{-1} Tyr at different temperatures

Table 4 Electrochemical Characteristics Derived from Figure 6

Solution	T (°C)	E_{corr} (mV/SCE)	I_{corr}(µA/cm^2)	bc(mV/dec.)	E_I(%)
HNO_3 (1M)	20	261	84.07	-162.78	-
	30	274	105.7	-143.37	-
	40	269	139.8	-148.72	-
	50	302	262.2	-147.62	-
HNO_3 (1M) + 10^{-3}M Tyr	20	111	15	-160	82
	30	174	59	-169	45
	40	192	89	-169	36
	50	252	194	-167	26

The effect of the temperature shows that the increase of corrosion rate is more pronounced with the rise of temperature for the blank solution. In the presence of Tyr, the corrosion current densities (I_{corr}) increase when the temperature rises from 20 to 50°C at 10^{-3} mol.L^{-1} of Tyr. The inhibition efficiency E(%) decreases from 82 to 26% with the temperature. This behaviour can be explained due to a reduction in the stability of adsorbed film at higher temperatures [10].The same result was found elsewhere **[**57].

Thermodynamic Activation Parameters

Thermodynamic activation parameters have an important role in understanding the inhibitive mechanism of organic inhibitors. Activation parameters such as: the activation of energies (E_a), the enthalpy of activation (ΔH_a), and the entropy of activation (ΔS_a) were calculated. The apparent activation energies for the copper dissolution process can be evaluated from the following relationship:

$$I_{corr} = A \exp\left(\frac{-E_a}{RT}\right)$$

$$I'_{corr} = A \exp\left(\frac{-E'_a}{RT}\right)$$

Where **A** is Arrhenius constant, $\mathbf{E_a}$ and $\mathbf{E_a'}$ are the activation energies for the corrosion in the presence and absence of the inhibitor, respectively. **T** is the absolute temperature in Kelvin and **R** is the universal gas constant. The logarithm of the corrosion rate of copper $\mathbf{I_{corr}}$ can be represented as straight-lines function of **1/T** (Arrhenius equation) in **Figure7** with slopes of $-E_a/R$. Corrosion kinetic parameters for the Tyr obtained from these graphs are given in **Table 5**. It is observed that the E_a value is increased in the presence of inhibitor that indicates the poorer performance of the compound at higher temperatures [43, 58].

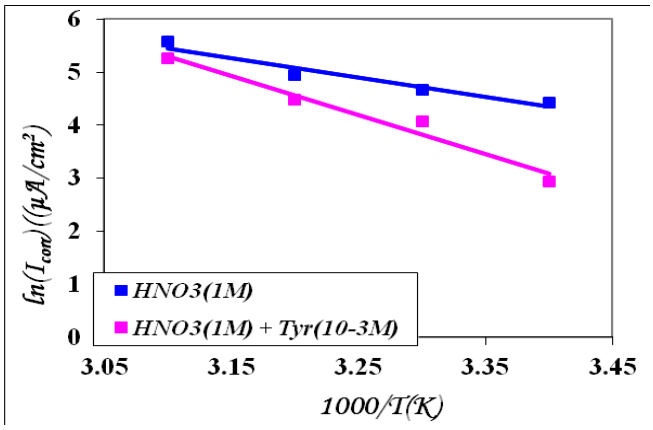

Figure 7 Arrhenius plots of copper in 1.0 mol/L HNO_3 without and with 10^{-3} mol.L^{-1} of Tyr

Table 5 The values of activation parameters E_a and ΔH° for copper in 1.0 mol.L^{-1} HNO_3 in the absence and the presence of Tyr at 10^{-3} mol.L^{-1}

Inhibiteur	E_a (Kj/mol)	ΔH° (Kj/mol)
HNO_3 (1M)	30.75	27.92
HNO_3 (1M) + Tyr (10^{-3}M)	61,34	58,64

The nature of the adsorption process can be clarified further if the heat of adsorption $\Delta H°_{ads}$ value is known. It has been shown that for $\Delta H°_{ads} < 10$ kJ/mol the adsorption is most probably physical in character, while for $\Delta H°_{ads} > 10$ kJ/mol chemisorption is expected [59]. The determination of $\Delta H°_{ads}$ may be deduced from the following relationship:

$$\mathrm{Ln}\left(\frac{I_{corr}}{T}\right) = -\frac{\Delta H°}{RT} + B$$

Where **h** is Planck's constant, **N** is Avogadro's number and **ΔH°** is the enthalpy of activation. The logarithm of the corrosion rate of copper $\mathbf{I_{corr}/T}$ is represented as straight-lines function of **1/T** in **Figure8** with slopes of –ΔH°/R.

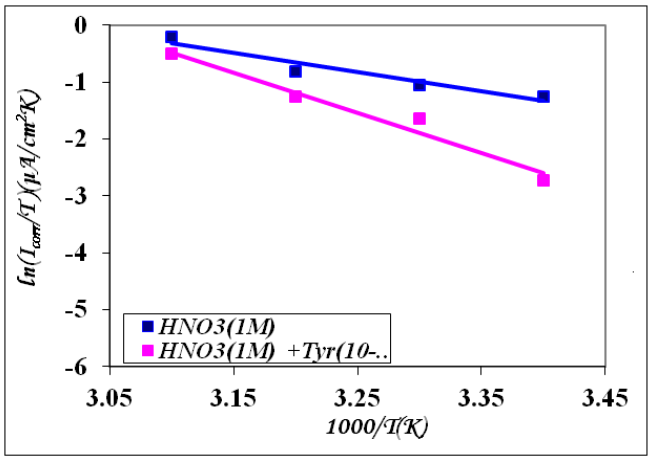

Figure 8 Transition state plots of copper in 1.0 mol.L^{-1} HNO_3 without and with 10^{-3} mol.L^{-1} of Tyr

Effect of Immersion Time

Table 6 shows the variation of the weight loss V_{corr} of copper at various times of immersion in 1 mol.L^{-1} HNO_3 at 20°C in the absence and presence of 10^{-3} mol. L^{-1} of Tyr. The examination of the data shows that the copper dissolution increased with time and reached a maximum value at 24h (**Figure 9**). In the presence of inhibitor, we observed that the attack of copper is highly reduced (Figure 9). The curve (**Figure 10**) obtained in the presence of Tyr shows that the inhibition efficiency (E_R%) increase with time. We note that E(%) attains 83% at 4h and decreases from 83% to 75% when the time rises from 4h to 24h at 10^{-3} mol.L^{-1} of Tyr.

Table 6 Corrosion rates (V_{corr}) of copper and inhibition efficiencies (E_R%) of Tyr at 10^{-3}M as function of immersion time

Solution	Durée d'immersion (h)	V_{corr} (mg.cm^{-2}.h^{-1})x10^{-3}	E_R (%)
HNO_3 (1M)	2	29	-
	4	54	-
	16	62	-
	24	236	-
HNO_3 (1M)	2	11	62
+	4	09	83
10^{-3}M Tyr	16	14	77
	24	58	75

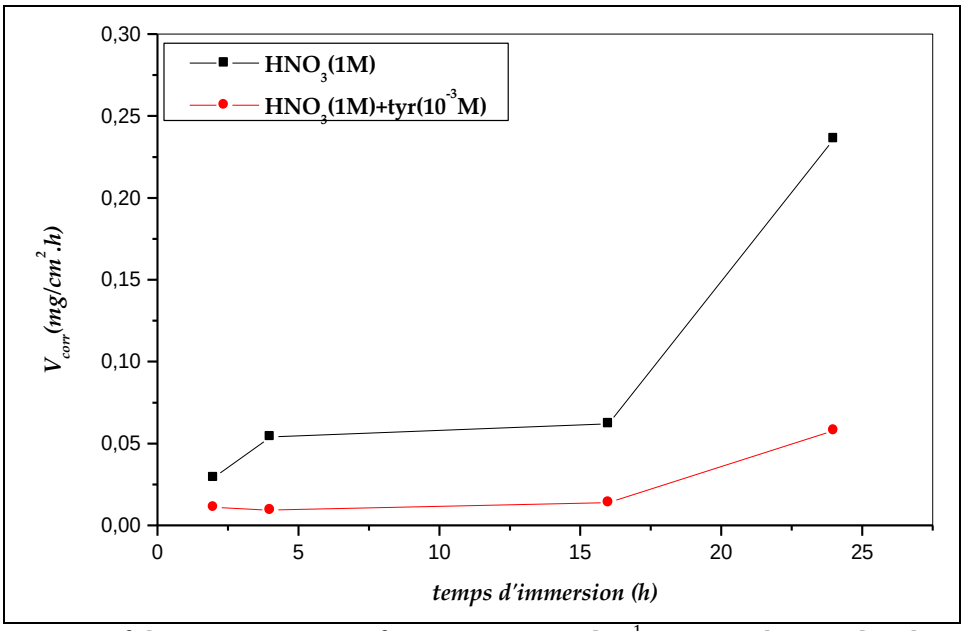

Figure 9 Time variation of the corrosion rates of copper in 1.0 mol.L^{-1} HNO_3 without and with Tyr at 10^{-3} mol.L^{-1}

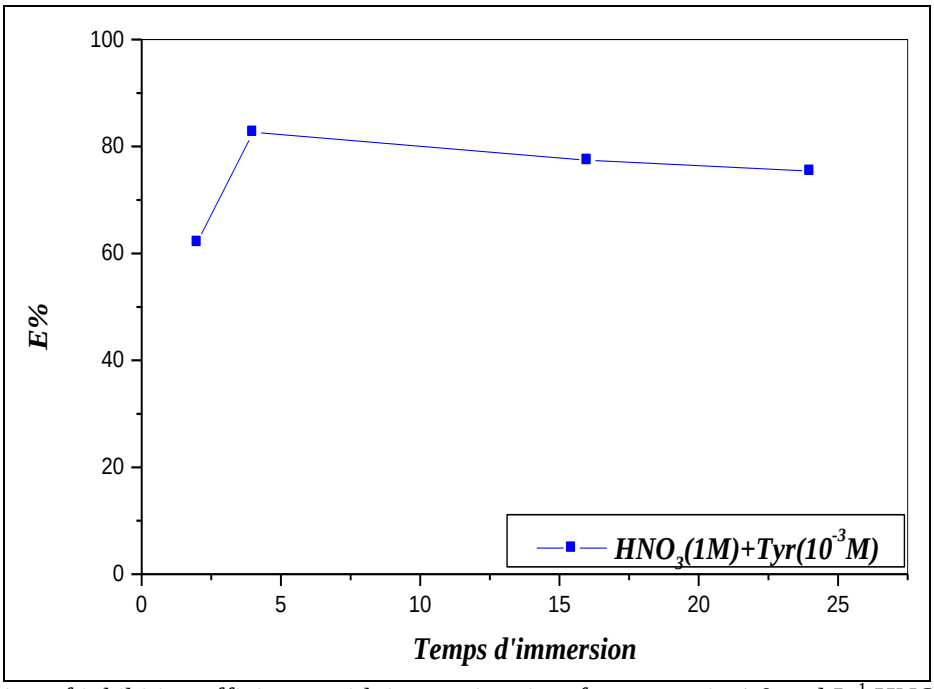

Figure 10 Variation of inhibition efficiency with immersion time for copper in 1.0 mol.L^{-1} HNO_3 containing 10^{-3} mol.L^{-1} of Tyr at 20°C.

SEM Measurements

Figure 11 shows the copper surface before corrosion and after immersion in nitric acid solution in the absence and presence of Tyr at 10^{-3} mol L^{-1} after 24h at 20°C. The results obtained are as shown in Figure 11(a), (b) and (c), respectively. In the absence of inhibitor (Figure 11(a**)**), the copper surface was damaged due to rapid corrosion attack in the nitric solution. Figure 11(c**)** indicate that in the presence of inhibitor the rate of corrosion is suppressed, as can be sen from the decrease of corroded areas. The metal surface is almost free from corrosion due to the formation of an insoluble complex on the surface of the metal [60-61]. In the presence of Tyr, the surface is covered by a layer of inhibitors which effectively controls the dissolution of copper.

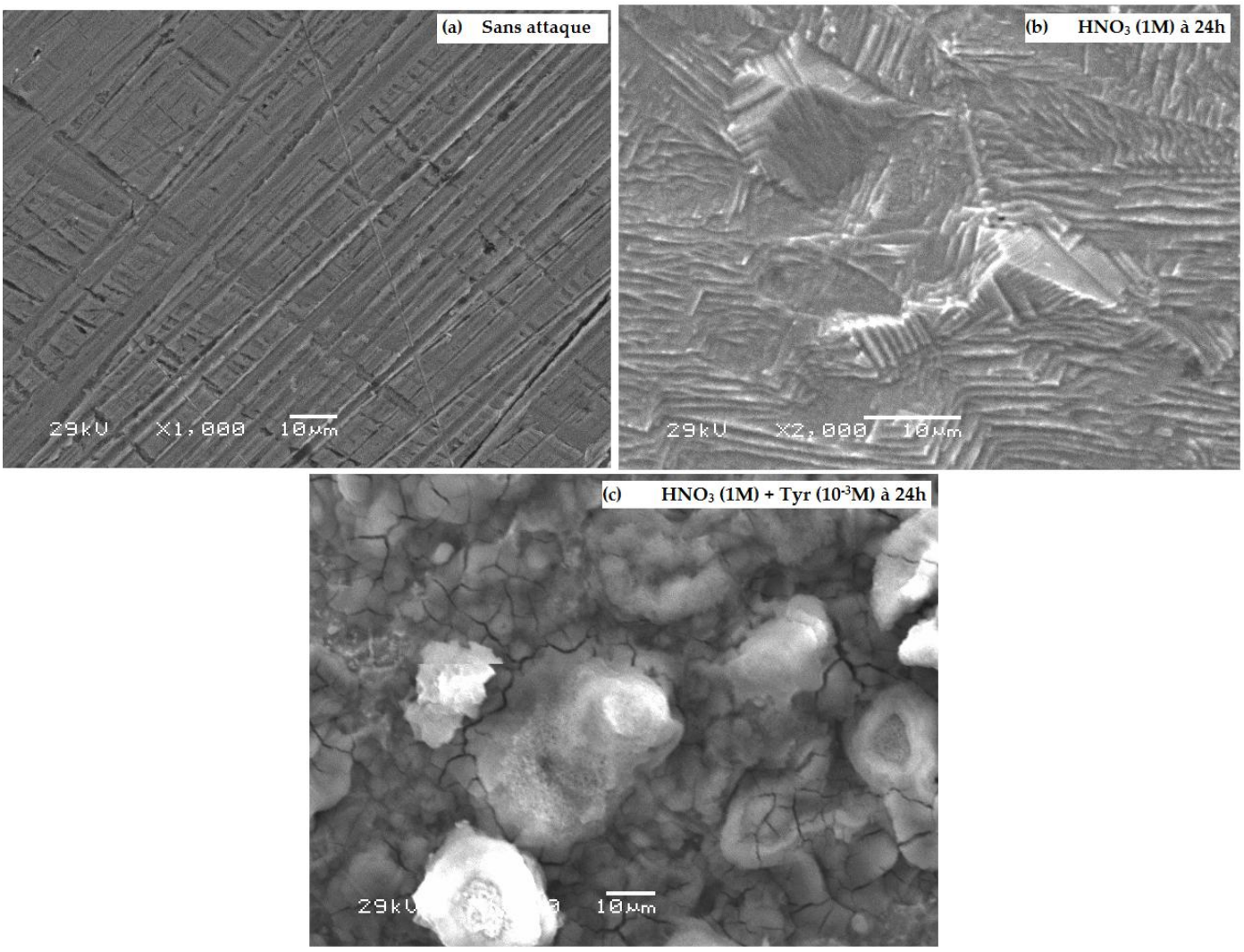

Figure 11 (a): SEM micrographs of copper surface: before immersion to solution of nitric acid. (**b**) SEM micrographs of copper surface: after exposition in a 1.0 mol.L^{-1} HNO_3 solution after 24 hours at 20°C. (**c**) SEM micrographs of copper surface: in the presence 10^{-3} mol.L^{-1} of Tyr after 24 hours at 20°C.

Quantum chemical calculation using semi empirical methods

Over the past decades the semi empirical molecular orbital methods have been widely used in computational studies. Semi empirical methods serve as efficient computational tools which can yield fast quantitative estimates for a number of properties [62]. Highest occupied molecular orbital energy (EHOMO) and lowest unoccupied molecular orbital energy (ELUMO) are very popular quantum chemical parameters. These orbitals, also called the frontier orbitals, determine the way the molecule interacts with other species. According to the frontier molecular orbital theory, the formation of a transition state is due to an interaction between the frontier orbitals (HOMO and LUMO) of reactants [63]. EHOMO is often associated with the electron donating ability of the molecule. High EHOMO values indicate that the molecule has a tendency to donate electrons to appropriate acceptor molecules with low energy empty molecular orbital. Increasing values of the EHOMO facilitate adsorption (and therefore inhibition) by influencing the transport process through the adsorbed layer [64-65]. ELUMO indicates the ability of the molecules to accept electrons. The lower values of the ELUMO, the more probable it is that the molecule would accept electrons. A low value of the energy band gap (ΔE = ELUMO - EHOMO) gives good inhibition efficiencies, because the energy to remove an electron from the last occupied orbital will be low [66].

Table 7 shows the quantum chemical calculation parameters (EHOMO, ELUMO, ΔE (ELUMO – EHOMO) which have been calculated and correlated with experimental results. From this Table it is evident that a correlation

exists between EHOMO and inhibition efficiency of the amino acids. The less negative EHOMO and the smaller ΔE (**Table 7**) reflect a great inhibition efficiency of the Tyr inhibitor [67-68].

Table7 The calculated quantum chemical parameters for Tyr

Tyr	E_{HOMO}/ev	E_{LUMO}/ev	ΔE/ev
AM1	-12,34	-4,54	7,80
MNDO	-12,46	-5,32	7,14

The inhibition efficiency of inhibitor compound is probably due to the presence of N and O atoms and phenyl in the molecular structure may increase the polarity and the adsorbability of inhibitors on the metal surface [1, 31, 55]. The optimum conformation of the protonated form of Try is shown in (**Figure 12**).

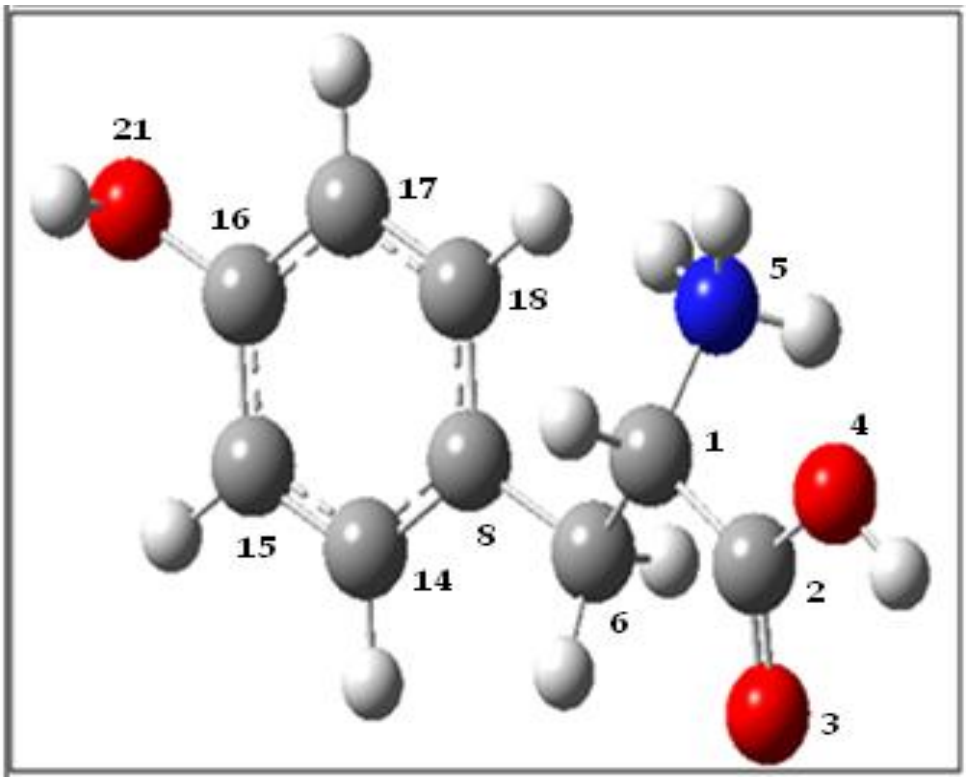

Figure 12 The optimum conformation of the protonated form of Tyr.

The values of the atomic charge are computed using the method AM1, and the values of the net atomic charge are presented in **Table 8**. A comparison of the calculated values shows that the net atomic charge is always more negative at the oxygen atom than at the nitrogen atom of Tyr. Furthermore, the electron density at the C_8 and C_{15} atoms is higher than the other atoms of the compound. So these negative atomic charges of oxygen (O_3, O_4 and O_{21}) and carbon (C_8 and C_{15}) atoms signify that the adsorption will be better through these atoms [69-70].

Table 8 Net atomic charges of Tyr compound calculated by the AM1 method

inhibitor	C_8	C_{14}	C_{15}	C_{16}	C_{17}	C_{18}	O_3	O_4	O_{21}	N_5
Tyr	-0,218	-0,091	-0,214	0,126	-0,147	-0,081	-0,253	-0,343	-0,222	-0,058

Conclusions

The following main conclusions are drawn from the present study:

- The protection efficiency of this inhibitor increases with the increase of the inhibitor concentration to attain 82% at 10-3 mol.L-1 and then decreases at higher concentrations.
- Polarisation measurements show that the Tyr acts as a cathodic inhibitor.
- The weight loss, linear polarisation resistance and polarisation curves were in good agreement.
- Tyr adsorb on the copper surface according to the Langmuir isotherm adsorption.
- The inhibition efficiency of Tyr is dependent on temperature and immersion time.
- Thermodynamic activation parameters reflect the endothermic nature dissolution process of copper.
- The SEM images confirm the protection of copper corrosion in nitric acid solution by Tyr.
- From quantum chemical calculations, Tyr has the lowest value of energy gap ΔE, reflect a great inhibition efficiency of this inhibitor.
- The adsorption of the Tyr on the copper surface occurs mostly through the lone pair of electrons of the heteroatoms (oxygen atoms) and π-electrons of the phenyl rings.

References

[1] Sherif EM, Park SM, Electrochim Acta 2006, 51, p4665.
[2] Barouni K, Bazzi L, Salghi R, Mihit M, Hammouti B, Albourine A, El Issami S, Mater Let 2008, 62, p3325.
[3] Zucchi F, Grassi V, Frignani A, Trabanelli G, Corros Sci, 2004, 46, p2853.
[4] Zarrouk A, Hammouti B, Dafali A, Zarrok H, Der Pharma Chemica, 2011, , p266.
[5] Sherif ESM, Erasmus RM, Comins JD, J Colloid Int Sci, 2007, 309, p470.
[6] Ashassi-Sorkhabi H, Majidi MR, Seyyedi K, Appl Surf Sci, 2004, 225, p176.
[7] Lalitha A, Ramesh S, Rajeswari S, Electrochim Acta, 2005, 51, p47.
[8] Sayed SY, El-Deab MS, El-Anadouli BE, Ateya BG, J Phys Chem, 2003,107, p5575.
[9] Qafsaoui W, Blanc C, Pebere N, Takenouti H, Srhiti A, Mankowski G, Electrochim Acta, 2002, 47, p4339.
[10] Olivares O, Likhanova NV, Gomez B, Navarrete J, Llanos-Serrano ME, Arce E, Hallen JM, Appl Surf. Sci, 2006, 252, p2894.
[11] Nuyuh N, Bottle SE, Notoya T, Trueman A, Hinton B, Schweinsberg DP, Corros Sci, 2002, 44, p1257.
[12] Gasparac R, Martin CR, Stupnis E ˇek-Lisac, J Electrochem Soc, 2000,147, p548.
[13] Geler E, Azambuja DS, Corros Sci, 2000, 42, p631.
[14] ZHANG DQ, GAO LX and ZHOU GD, J Appl Electrochem, 2003, 33, p361.
[15] Yu P, Liao DM, Luo YB, Chen ZG, Corros, 2003, 59, p314.
[16] Stupnisek-Lisac E, Brnada A, Mance AD, Corros Sci, 2000, 42, p243.
[17] Ashassi-Sorkhabi H, Ghasemi Z, Seifzadeh D, Appl Surf Sci, 2005, 249, p408.
[18] Zhang DQ, Gao LX, Zhou GD, J Appl Electrochem, 2005, 35, p1081.
[19] Matos JB, Pereira LP, Agostinho SML, Barcia OE, Cordeiro GGO, D'Elia E, J Electroanal Chim, 2004, 570, p91.
[20] Kertit S, Salghi R, Bazzi L, Hammouti B, Bouchtart A, Ann Chim Sci Mat, 2000, 25, p187.
[21] Eddy NO, J Advanced Research, 2011, 2, p35.
[22] Gece G, Bilgiç S, Corros Sci, 2010, 52, p3435.
[23] Zhang DQ, Cai QR, He XM, Gao LX, Zhou GD, Mater Chem Phys, 2008, 112, p353.
[24] HA Zheng, Zhang DQ, Xing J, Corros Protection, 2007, 28, p607.
[25] Moretti G, Guidi F, Corros Sci, 2002, 44, p1995.
[26] Barouni K, Kassale A, Albourine A, Jbara O, Hammouti B, Bazzi L, J Mater Environ Sci, 2014, 5, p456.
[27] [27] Kesavan D, Gopiraman M, Sulochana N, Chem Sci Rev Lett, 2012,1, p1
[28] Barouni K, Kassale A, Bazzi L, Salghi R, Hammouti B, Albourine A, El Issami S, Jbara O, Bouachrine M, Res Chem Intermediates, DOI 10.1007/s11164-012-1016-9.
[29] Raja P B, Sathuraman M G, Mater Lett, 2009, 62, p113.
[30] Al-Karafi FM, Badawy WA, Ind J Chem Technol, 1996, 3, p212–218.
[31] Barouni K, Kassale A, Bazzi L, Albourine A, J Chem Bio Phy Sci Sec A, 2014, 4, p3140.
[32] El-Abedin SZ, J Appl Electrochem, 2001, 31, p711.
[33] Zarrouk A, Hammouti B, Zarrok H, Salghi R, Dafali A, Bazzi L, Bammou L, Al-Deyab SS, Der Pharma Chemica, 2012, 4, p337.

[34] Stupnisek-Lisac E, Gazivoda A, Madzarac M, Electrochim Acta, 2002, 47, p4189.
[35] Zhang DQ, Cai Qi Rui, Xian-Ming Heb, Gaoa LX, Gui Soon Kim, Mater Chem Phys, 2009, 114, p612.
[36] Oguzie EE, Y Li, Wang FH, J Colloid Interface Sci, 2007, 310, p90.
[37] Özcan M, Karadag F, Dehri I, Colloids Surf Physicochem Eng Aspects, 2008, 316, p55.
[38] Yurt A, Bereket G, Ogretir C, J Mol Struct THEOCHEM, 2005, 725, p215.
[39] Bereket G, Ogretir C, Yurt A, J Mol Struct (THEOCHEM), 2001, 571, p139.
[40] Dewar M J S, Zoebish E G, Healy E F, Stewart J J P, J Am Chem Soc, 1985,107, p3902.
[41] Dewar M J S, Thiel W, J Am Chem Soc, 1977, 99, p4907.
[42] Stewart JJP, Seiler FJ, MOPAC Version 60, Research Laboratory, United State Air Force Academy, 1990 Co 80840.
[43] Bouklah M, Attayibat A, Kertit S, Ramdani A, Hammouti B, Appl Surf Sci 2005, 242, p399.
[44] Al-Mobarak NA, Khaled KF, Abdel-Azim KM, J Mater Environ Sci 2010, 1, p9
[45] Bentiss F, Gassama F, Barbry D, Gengembre L, Vezin H, Lagrenée M, Traisnel M, Appl Surf Sci, 2006, 252, p2684.
[46] Abed Y, Kissi M, Hammouti B, Taleb M, Kertit S, Prog Org Coat, 2004, 50, p144.
[47] Morad M, Hermas A, Aal M, J Chem Technol Biotechnol, 2002, 77, p486.
[48] Amin MA, Khaled KF, Corros Sci, 2010, 52, p1194
[49] Ghasemi Z, Tizpar A, Appl Surf Sci, 2006, 252, p3667
[50] Langmuir I, J Am Chem Soc, 1947, 39, p1848.
[51] Larabi L, Benali O, Mekelleche SM, Harek Y, Appl Surf Sci, 2006, 253, p1371.
[52] Bouklah M, Hammouti B, Lagrene M, Bentiss F, Corros Sci, 2006, 48, p2831.
[53] Ye XR, Xin XQ, Zhu JJ, Xue ZL, Appl Surf Sci, 1998, 135, p307.
[54] Tebbji K, Hammouti B, Oudda H, Ramdani A, Benkadour M, Appl Surf Sci, 2005, 252, p1378.
[55] Tebbji K, Bouabdellah I, Aouniti A, Hammouti B, Oudda H, Benkaddour M, Ramdani A, Mater Lett, 2007, 61, p799.
[56] Bouklah M, Ouassini A, Hammouti B, El Idrissi A, Appl Surf Sci, 2005, 250, p50.
[57] Tebbji K, Aouniti A, Benkaddour M, Oudda H, Bouabdallah I, Hammouti B, Ramdani A, Progress Org Coatings, 2005, 54, p170.
[58] Popova A, Sokolova E, Raicheva S, Christov M, Corros Sci, 2003, 45, p33.
[59] Elayyachy M, Hammouti B, El Idrissi A, Aouniti A, Port Electrochim Acta, 2011, 29, p57.
[60] Anthony S, Sahaya R, Rajendran S, J Electrochem Sci Eng, 2012, 2, p91.
[61] Gopi D, Manimozhi S, Govindaraju KM, Manisankar P, Rajeswari S, J Appl Electrochem, 2007, 37, p439.
[62] Gece G, Corros Sci, 2008, 50, p2981.
[63] Fukui K, Theory of Orientation and Stereose-lection, Springer-Verlag, New York, 1975
[64] Ashassi-Sorkhabi H, Shaabani B, Seifzadeh D, Electrochim Acta, 2005, 50, p3446.
[65] Ozcan M, Dehri I, Erbil M, Appl Surf Sci, 2004, 236, p155.
[66] Khalil N, Electrochim Acta, 2003, 48, p2635.
[67] Gece G, Bilgic S, Turksen O, Mater Corros, 2009, 60, p9999.
[68] Gece G, Corros Sci, 2008, 50, p2981.
[69] Karthikeyan S, Jeeva PA, Narayanan S, Int J Chem Tech Res, 2013, 5, p1897.
[70] Stoyanova A, Petkova G, Peyerimhoff SD, Chem Phys, 2002, 279, p1.

Publication History
Received 09th Apr 2016
Accepted 20th May 2016
Online 30th Oct 2016